Original scientific paper

VIBRATION PHENOMENA INDUCED BY PULSED LASER HEATING OF MICROMECHANICAL CANTILEVER: INFLUENCE OF LASER-PULSE TEMPORAL SHAPE

UDC 534.23:772.96

Slobodanka Galović[1], Katarina Đorđević[1], Mladena Lukić[2], Dalibor Chevizovich[1]

[1]University of Belgrade, Vinča Institute of Nuclear Sciences, Belgrade, Serbia
[2]University of Nis, Faculty of Occupational Safety in Niš, Serbia

ORCID iDs:	Slobodanka Galović	https://orcid.org/0000-0002-6728-8868
	Katarina Đorđević	https://orcid.org/0000-0002-1397-8011
	Mladena Lukić	https://orcid.org/0000-0003-1105-3637
	Dalibor Chevizovich	https://orcid.org/0000-0001-7688-3792

Abstract. *Illumination-induced vibrational phenomena can significantly affect the mechanical behavior of micro-mechanical sensors (MEMS) and, consequently, the noise performance of detectors based on these sensors. In this paper, we study thermoelastic deflection induced by photothermal heating of a solid micro-mechanical cantilever illuminated by a short square laser pulse. An analytical-numerical technique based on the Laplace transform is employed to calculate the spectral function of lateral deflection. The results indicate that the profile of laser-induced vibrations depends on the temporal shape of the excitation optical pulse. The square pulse enhances the increasing trend of the high-frequency lateral vibration amplitude peak if cantilever thickness increases suggesting the possibility of size-dependent engineering of the properties of detectors utilizing micro-mechanical cantilevers.*

Key words: *photothermal effect, generalized thermoelasticity, cantilever, micro resonator, nano electro-mechanical systems*

1. INTRODUCTION

Laser-induced heating of a solid, also known as the photothermal (PT) effect [1–3], causes a temperature gradient within the illuminated sample, altering the temperature profile and, consequently, generating expansions and contractions in the optically excited sample [4–6]. This mechanism has attracted considerable attention due to the extensive application of lasers

in material processing and the non-destructive detection and characterization of various materials and devices, including biomedical diagnostics [7–13]. Laser-induced vibrations of thin cantilevers have also gained significant attention because of their technological applications in Micro-Electro-Mechanical Systems (MEMS) and Nano-Electro-Mechanical Systems (NEMS) [14–17].

The analysis of thermoelastic displacements requires examining the coupled temperature and deformation fields [5]. In the case of ultra-short-pulsed laser heating, the high-intensity energy flux and ultra-short laser beam duration create situations where very large thermal gradients or ultra-high heating speeds may occur at the boundaries. In such cases, as noted by many investigators, the classical Fourier model, which implies an infinite propagation speed of thermal energy, is no longer valid [17–23]. The non-Fourier effect of heat conduction accounts for thermal relaxation time in the relationship between heat flux and the temperature gradient, thereby resolving this contradiction. For this reason, a generalized model of the thermoelastic problem, known as the Lord-Shulman model, was proposed. It introduces a hyperbolic theory of heat conduction that incorporates the non-Fourier effect [24]. This model has been applied in many studies of thermoelastic deformation induced by modulated laser beams or pulsed laser irradiation [25–27].

In the literature, one can find studies addressing optically generated vibrations of a thin cantilever of finite length illuminated by pulses with smooth rising and falling edges, such as Gaussian and non-Gaussian time profiles of short duration [16,27]. However, in many applications of semiconducting micro-mechanical devices, the time dependence of the excitation beam is better described by short square pulses or a series of such pulses [28–31]. Therefore, this paper derives a model of thermoelastic vibrations in a micro-mechanical cantilever, assuming that the time dependence of the optical excitation can be described by a short square pulse.

Based on the derived model, the spectral function of the lateral displacement profile for low and high harmonics is calculated and analyzed. The dependence of the high-frequency amplitude peak of midpoint deflection on the cantilever thickness is also investigated. Finally, the most important conclusions are presented.

2. MATHEMATICAL FORMULATION OF THE PROBLEM

We consider the micro-mechanical resonator (MMR) illustrated in Fig. 1, whose length is denoted as L, and whose cross-section is rectangular, with linear dimensions b and h that are much smaller than the sample length L.

The initial temperature distribution $T(x, y, z, t = 0)$ is assumed to be equal to the environmental temperature T_0. From the moment $t = 0$, the upper surface of the resonator ($z = h/2$) is uniformly irradiated by a short laser pulse.

$$S(t) = S_0 f(t) = S_0(h(t) - h(t - t_p)) \tag{1}$$

where t_p is the duration of a laser pulse and S_0 is the laser irradiance (total energy carried by a laser pulse per unit of cross section of the sample per unit of time).

Absorbed electromagnetic energy generates thermal source along the $z-$ axis (photothermal effect) $Q(z,t)$ [27]:

$$Q(z,t) = S_0 R_a e^{\dfrac{z - \dfrac{h}{2}}{\delta}} f(t) \tag{2}$$

where δ is the absorption depth of electromagnetic energy (inverse coefficient of optical absorption) and R_a is the coefficient of optical reflection of irradiated surface.
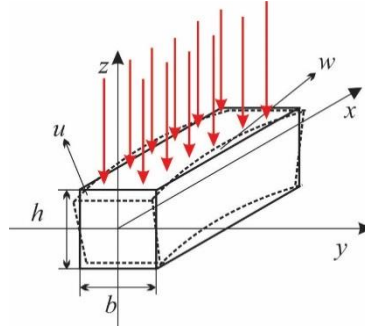

Fig.1 Geometry of the problem

Since the heat source depends on only one spatial coordinate ($z$coordinate), the photothermally induced heat transfer within the micro-mechanical resonator (MMR) can be described as a one-dimensional problem. In this case, the non-Fourier thermal conduction that includes the thermoelastic coupling term has the following form [24]:

$$\rho c_v \frac{\partial \vartheta}{\partial t} + \tau_0 \rho c_v \frac{\partial^2 \vartheta}{\partial t^2} + \beta \tau_0 \frac{\partial e}{\partial t} + \tau_0 \beta T_0 \frac{\partial^2 e}{\partial t^2} - k \frac{\partial^2 \vartheta}{\partial z^2} = Q + \tau_0 \frac{\partial Q}{\partial t}, \tag{3}$$

where $\vartheta(x,z,t) = T(x,z,t) - T_0$ is the temperature increment, $e = \dfrac{\partial u}{\partial x} + \dfrac{\partial v}{\partial y} + \dfrac{\partial w}{\partial z}$ is

volumetric strain, coefficient β is defined by $\beta = E\alpha_T(1-2v)$ in which v is Poisson's ratio, E is Young's modulus, and α_T is coefficient of linear expansion of the sample, c_v is the heat capacity, ρ is the mass density of the sample, k is heat conductivity, and τ_0 is the thermal relaxation time (this parameter has not yet been measured in any material at room temperature, and estimates of its value for semiconductors and dielectrics range from the order of magnitude of microseconds to the order of picoseconds [27,32,33], meaning that the influence of this parameter should be taken into account for laser pulses of picosecond duration.) In Eq. 3, we neglected the influence of photogenerated electrons and electron-phonon interactions on sample heating [34–37]. With u, v, w are denoted the displacements in the direction of x, y, and z-axis, respectively, Fig. 1.

By considering that there is no heat flow across the upper and lower surfaces of MMR, the following boundary conditions can be defined:

$$\frac{\partial \vartheta(x,z,t)}{\partial z}\Big|_{z=h/2} = 0 \tag{4}$$

the photothermally generated displacement of MMR is described by using the usual Euler-Bernoulli assumption [27]:

$$u = -z \frac{\partial w}{\partial x}, \ v = 0, \ w(x, y, z, t) = w(x, t), \tag{5}$$

where w the lateral deflection (see Fig. 1).

The differential equation of thermally induced lateral deflection w of the sample can be written in the form:

$$EI \frac{\partial^4 w}{\partial x^4} + \rho bh \frac{\partial^2 w}{\partial t^2} + EI \alpha_T \frac{\partial^2 M_T}{\partial x^2} = 0, \tag{6}$$

where M_T is thermal moment, which is defined as:

$$M_T = \frac{12}{h^3} \int_{-h/2}^{h/2} z\vartheta(x, z, t) dz \tag{7}$$

and I is the moment of inertia for the structure illustrated in Fig. 1, $I = bh^3/12$.

For a very thin resonator, Eq. 7, can be reduced to [27]:

$$M_T = -\frac{1}{p^2} \int_{-h/2}^{h/2} \frac{12}{h^3} \frac{\partial^2 \vartheta}{\partial z^2} z dz, \tag{8}$$

where $p = \pi / h$.

By using Eqs. 2, 3 and 6, 8, the generating equations for the coupled thermoelastic problem can be obtained as follows:

$$EI \frac{\partial^2 w}{\partial x^4} + \rho bh \frac{\partial^2 w}{\partial t^2} + EI \alpha_T \frac{\partial^2 M_T}{\partial x^2} = 0 \tag{9}$$

$$k \left(\frac{\partial^2 M_T}{\partial x^2} - p^2 M_T \right) - C_v \frac{\partial M_T}{\partial t} + T_\beta \frac{\partial^3 w}{\partial x^2 \partial t} - \tau_0 C_v \frac{\partial^2 M_T}{\partial t^2} + \tau_0 T_\beta \frac{\partial^4 w}{\partial x^2 \partial t^2} + \frac{6 R_a S_0 a_\delta \Gamma(t)}{h^2} = 0 \tag{10}$$

where: $C_v = \rho c_v$, $T_\beta = T_0 \beta$, $a_\delta = \dfrac{(1 + 2a) + (1 - 2a)e^{\frac{1}{a}}}{e^{\frac{1}{a}}}$, $a = \delta / h$, and

$$\Gamma(t) = f(t) + \tau_0 \frac{\partial f(t)}{\partial t}. \tag{11}$$

The problem described by Eqs. 3, 8, and 9-11 with zero initial conditions is a standard problem, the solution of which, for different methods of strengthening a thin micro-cantilever (Fig. 1), describes the lateral deflection profile and its dependence on time. The temporal shape of the excitation pulse $f(t)$ affects the lateral deflection through the function $\Gamma(t)$ in Eq. 10. In the literature, a similar description of the problem can be found for optical

excitation in the form of an asymmetric Gaussian function [27]. The problem described in this section is more general because it includes any time dependence of the excitation pulse.

In this paper, the problem of lateral deflection is solved under the assumption that the sample is clamped on both sides:

$$\frac{\partial w(x,z,t)}{\partial x}\Big|_{x=0} = \frac{\partial w(x,z,t)}{\partial x}\Big|_{x=L} = 0, \quad w(x=0,z,t) = w(x=L,z,t) = 0, \tag{12}$$

and that the moment of temperature is equal to zero in the places where the sample is clamped:

$$M_T(x=0,t) = M_T(x=L,t) = 0. \tag{13}$$

We did the calculation by introducing dimensionless coordinates

$$\zeta = \frac{x}{L}, \quad \tau = \frac{vt}{L}, \tag{14}$$

where $v = \sqrt{\dfrac{E}{\rho}}$ is the longitudinal speed of propagation of elastic deformation.

We also introduced two dimensionless variables: dimensionless deflection $W(\zeta,\tau)$ and dimensionless thermal moment, $\Theta(\zeta,\tau)$:

$$W(\zeta,\tau) = \frac{w(x,t)}{L}, \quad \Theta(\zeta,\tau) = \alpha L M_T(x,t). \tag{15}$$

Since the problem described by Eqs. 3, 8, 9, and 11 is linear in time, it can be solved by the application of Laplace transform on time dependence variables. This transform, as well as dimensionless coordinates and considered variables, reduce the problem to two ordinary differential equations in a complex domain:

$$\frac{d^4\overline{W}(\xi)}{d\xi^4} + \overline{A}_1\overline{W}(\xi) + \frac{d^2\overline{\Theta}(\xi)}{d\xi^2} = 0, \tag{16}$$

$$\frac{d^2\overline{\Theta}(\xi)}{d\xi^2} - \overline{A}_2\overline{\Theta}(\xi) + \overline{A}_3\frac{d^2\overline{W}(\xi)}{d\xi^2} = -A_4\overline{G}(s), \tag{17}$$

with zero boundary conditions (see Eqs. 12 and 13). In the above equations, the bar above symbols is introduced to denote variables and coefficients dependent on the complex frequency s, and $G(s)$ denotes the Laplace transformation (spectral function) of the function $\Gamma(t)$, which depends on the temporal shape of the optical excitation (Eq. 11).

Coefficients $\overline{A}_1 - \overline{A}_3$ are complex quantities that depend on the dimensions and properties of the sample:

$$\overline{A}_1 = \frac{12L^2}{h^2}s^2, \quad \overline{A}_2 = \frac{\tau_0 c_v E}{k}s^2 + \frac{c_v \rho v L}{k}s + p^2 L,$$

$$\overline{A}_3 = \frac{\tau_0 \alpha_T T_0 \beta E}{\rho k}s^2 + \frac{\alpha_T T_0 \beta v L}{k}s, \tag{18}$$

while the coefficient A_4 is real and equal to:

$$A_4 = \frac{6R_a S_0 \alpha_T L^3 \tau_0 a_\delta}{kh^2} \; . \tag{19}$$

If the second derivative of the dimensionless moment from Eq. 16 is replaced in Eq. 17, the expression for the generalized moment is obtained:

$$\bar{\Theta}(\xi) = -\frac{1}{\bar{A}_2}\frac{d^4\bar{W}(\xi)}{d\xi^4} - \frac{\bar{A}_1}{\bar{A}_2}\bar{W}(\xi) + \frac{\bar{A}_3}{\bar{A}_2}\frac{d^2\bar{W}(\xi)}{d\xi^2} + \frac{A_4}{\bar{A}_2}\bar{G}(s) \, , \tag{20}$$

which, by double differentiation and substitution in Eq.16, gives the differential equation that describes the lateral deflection along the dimensionless axis ξ (in the x-axis direction, Fig. 1):

$$\frac{d^6\bar{W}(\xi)}{d\xi^6} + \bar{a}\frac{d^4\bar{W}(\xi)}{d\xi^4} + \bar{b}\frac{d^2\bar{W}(\xi)}{d\xi^2} + \bar{c}\bar{W}(\xi) = 0 \tag{21}$$

where the coefficients in differential equation Eq. 21 are defined by the following expressions:

$$\bar{a} = -(\bar{A}_2 + \bar{A}_3) \; , \quad \bar{b} = \bar{A}_1 \; , \quad \bar{c} = -\bar{A}_1 \bar{A}_2 \, . \tag{22}$$

From Eqs. 21 and 22, one could mistakenly conclude that the lateral deflection does not depend on the irradiance, the temporal shape, and the duration of the excitation optical pulse, because neither the coefficient A_4 nor the function $G(s)$ appears anywhere. However, the resulting differential equation indicates that only the form of the fundamental solutions will be the same for any irradiance and for any time-dependent form of excitation, including a simple periodic modulated optical beam. The total solution, which represents a linear combination of the fundamental solutions, depends on the coefficients by which the fundamental solutions are multiplied. These coefficients, through the boundary conditions, depend on the irradiance, the temporal shape of the optical excitation, and the length of its duration.

The solution of linear homogeneous differential equation of the sixth order Eq. 21 can be found in the literature [27,38] and the solution procedure will not be presented here. This solution is given by a linear combination of fundamental solutions:

$$\bar{W}(\xi) = \sum_{j=1}^{3} (C_j e^{-\lambda_j \xi} + C_{j+3} e^{\lambda_j \xi}) \tag{23}$$

where λ_j are roots of characteristic equation for differential equation Eq. 21:

$$\lambda_1^2 = -P\eta - Q\eta^2 - \frac{\bar{a}}{3} \; , \quad \lambda_2^2 = -Q\eta - P\eta^2 - \frac{\bar{a}}{3}, \quad \lambda_3^2 = -P - Q - \frac{\bar{a}}{3} \tag{24}$$

Parameters A, P, Q, and η are related with complex coefficients of Eq.21 as follows:

$$P = \left[\frac{1}{2}\left(\bar{q} + \sqrt{\bar{q}^2 + 4\bar{p}^3}\right)\right]^{1/3} \; , \quad Q = \left[\frac{1}{2}\left(\bar{q} - \sqrt{\bar{q}^2 + 4\bar{p}^3}\right)\right]^{1/3} \, ,$$

$$\bar{p} = \frac{\bar{b} - \bar{a}^2/3}{3} \; , \quad \bar{q} = \bar{c} - \frac{\bar{a}\bar{b}}{3} + \frac{2}{27}\bar{a}^3 \; , \quad \eta = (-1 + i\sqrt{3})/2 \, . \tag{25}$$

By replacing Eq. 23 in 20, the solution for the dimensionless moment is also obtained:

$$\bar{\Theta}(\xi) = -\frac{1}{\bar{A}_2}\left[\sum_{j=1}^{3}\bar{K}_j(\bar{C}_j e^{-\lambda_j\xi} + \bar{C}_{j+3}e^{\lambda_j\xi}) - A_4\bar{G}(s)\right] \tag{26}$$

Where constants K_j are defined by the following expression:

$$K_j = \lambda_j^4 - \bar{A}_3\lambda_j^2 + \bar{A}_1 \tag{27}$$

As can be seen from the Eq. 26, the thermal moment depends on the irradiance, temporal shape, and duration of optical excitation directly, through the particular solution, but also indirectly, through the constants C_j.

The constants C_j can be determined by substituting Eqs. 23 and 26 into zero boundary conditions and solving the following matrix equation:

$$\begin{bmatrix} C_1 \\ C_2 \\ C_3 \\ C_4 \\ C_5 \\ C_6 \end{bmatrix} = \begin{bmatrix} 1 & 1 & 1 & 1 & 1 & 1 \\ e^{-\lambda_1} & e^{-\lambda_2} & e^{-\lambda_3} & e^{\lambda_1} & e^{\lambda_2} & e^{\lambda_3} \\ -\lambda_1 & -\lambda_2 & -\lambda_3 & \lambda_1 & \lambda_2 & \lambda_3 \\ -\lambda_1 e^{-\lambda_1} & -\lambda_2 e^{-\lambda_2} & -\lambda_3 e^{-\lambda_3} & \lambda_1 e^{\lambda_1} & \lambda_2 e^{\lambda_2} & \lambda_3 e^{\lambda_3} \\ K_1 & K_2 & K_3 & K_1 & K_2 & K_3 \\ K_1 e^{-\lambda_1} & K_2 e^{-\lambda_2} & K_3 e^{-\lambda_3} & K_1 e^{\lambda_1} & K_2 e^{\lambda_2} & K_3 e^{\lambda_3} \end{bmatrix}^{-1} \begin{bmatrix} 0 \\ 0 \\ 0 \\ 0 \\ A_4\bar{G}(s) \\ A_4\bar{G}(s) \end{bmatrix} \tag{28}$$

By numerical solving Eq. 28 and replacing the obtained constants in Eq. 23, we obtained the spectral functions of lateral displacement for short square optical pulse.

3. RESULTS AND DISCUSSIONS

We analyze the thermoelastic displacement excited by a square laser pulse of short duration for MMR made of silicon. The material parameters are given in Tab. 1 [27]. We take, as it was done in [27], that the aspect ratios of MMR are fixed as $L/h = 10$ and $b/h = 0.5$. The time duration of laser pulse is $t_p = 2$ps and the intensity of laser pulse is $S_0 = 10^{11}$ W/m^2. Parameter R_a depends on the material of the resonator and wavelength of laser beam. We take that $R_a = 0.5$.

Table 1 Material parameters used in calculation

Properties	Denotations	Value
Young modul	E	169 GPa
Mass density	ρ	2330 kg/m^3
Heat capacity	c_v	713 J/kgK
Coefficient of linear expansion	α_T	2.59 x10^{-6} 1/K
Poisson's ratio	v	0.22
Thermal conduction	k	156 W/mK

The Laplace transform of time dependence of heat source in Eq. 1 generated by square pulse is given by [40]:

$$G(s) = L\{\Gamma(t)\} = \left(\frac{1}{s} + \tau_0\right)(1 - e^{-st_p}) \qquad (28)$$

The calculated distribution of spectral function of dimensionless lateral deflection along the dimensionless axis normal to the direction of optical excitation (Eqs. 23, 27, 28) is illustrated in Fig. 2 for a few harmonics.
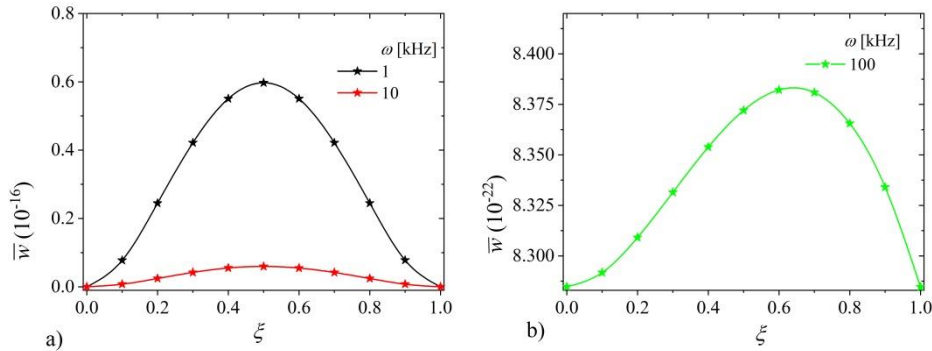

Fig. 2 a) The distribution of lateral deflection along the axis normal to the direction of optical excitation for following harmonics $f = 1$ kHz (black line), $f = 10$ kHz (red line), and b) $f = 100$ kHz (green line)

As can be seen from Figs. 2a and 2b, the maximum deflection (deflection peak) appears at the midpoint of the micro-cantilever for all harmonic excitation. This peak decreases when the frequency of harmonic increases. The form of lateral deflection depends on the frequency of harmonics: for lower harmonics, this form is symmetric in relation to the midpoint ($\xi = 0.5$, $x = L/2$) but for higher harmonic, this form becomes asymmetric due to the influence of spectral function of heat source induced by optical excitation, Eq. 28. It means that the temporal shape of optical excitation influences to distribution of lateral deflection.

High-frequency micro-cantilever vibrations are utilized in various types of oscillators and the development of different methods for non-destructive testing of materials [28,39]. Figure 3 shows the dependence of the midpoint amplitude of lateral vibrations (amplitude peak) on the frequency of the excitation harmonics.
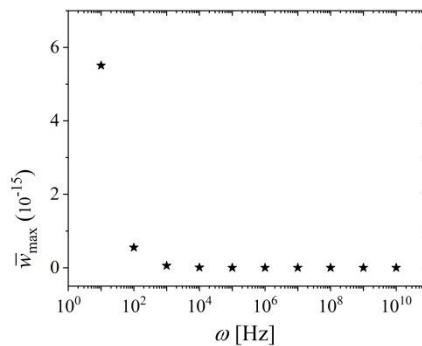

Fig. 3 The spectral function of midpoint lateral deflection

As shown in Fig. 3, the deflection peaks decrease rapidly with an increase in the frequency of the excitation harmonics, indicating that high-frequency vibrations generated by short optical excitation can be neglected.

Based on the derived model for the spectral function of the sample deflection (Eq. 23) the height of maximal deflection amplitude (peak of deflection) is calculated $f = 100$ kHz and its dependence on sample thickness h is shown in Fig. 4.
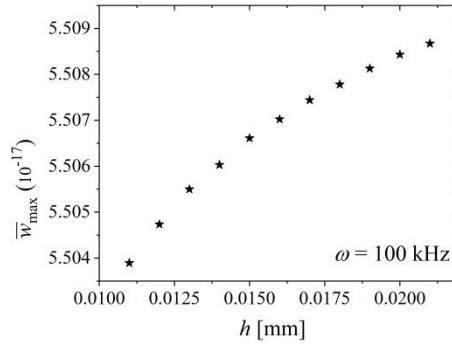

Fig. 4 The peak of deflection for samples of different thicknesses

Figure 4 shows a trend of increasing amplitude of the high-frequency peak of lateral deflection with increasing sample thickness, consistent with the model presented in [39] for a thin semiconducting disk excited by a high-frequency square pulse train, and contrary to the results presented in [27] for a micro-cantilever excited by a short non-Gaussian pulse. This indicates that the temporal shape of the excitation pulse affects this trend.

By applying the numerical inverse Laplace transform to the spectral function of dimensionless lateral displacement in Eq. 23, one can obtain the time-domain displacement for various temporal shapes of optical excitation. We attempted to solve the inverse Laplace transform for a square laser pulse of duration t_p (Eq. 1) numerically, using the MATLAB function INVLAP. However, this function did not yield good results for high-resolution changes in the dimensionless time coordinate because the sharp optical profile causes a steep wavefront of thermo-elastic deformation [41].

A detailed analysis of the impact of the square optical pulse on the time-dependent behavior of the temperature moment and lateral deflection requires the development of a numerical algorithm for solving the inverse Laplace transform for functions with sharp fronts [41], which is the subject of our further research.

4. Conclusions

In this paper, the model of photothermally induced vibration of lateral deflection is derived. The model is based on the Lord-Shulman theory of thermoelastic vibrations with the Euler-Bernoulli approximation. The derived model is more general than those in the literature because it includes any time-dependent optical excitation, enabling the study of the influence of the temporal shape of optical excitation on the vibrational characteristics of the deflection of micro-cantilevers.

Based on the derived model, the vibrational characteristics of the deflection of an Euler-Bernoulli micro-cantilever induced by a short square laser pulse are analyzed. The obtained results indicate that the spatial profile of laser-induced vibrations depends on the frequency spectrum of the excitation and, consequently, on the temporal shape of the laser pulse. The lateral vibrational peaks are scale-dependent, independent of the temporal shape of the laser pulse, but this shape influences the trend of either increase or decrease. For a square laser pulse, as the sample thickness increases, the peak deflection increases, indicating the possibility of size-dependent engineering of the high-frequency properties of various detectors that utilize micro-mechanical cantilevers.

Both the analysis of the frequency spectrum of the temperature moment based on the derived model and the time-domain analysis of lateral vibrations for various temporal shapes of the laser pulse are subjects of our ongoing investigations.

REFERENCES

1. Rosencwaig, A., Gerscho, A. Theory of the photoacoustic effect with solids. J. Appl. Phys., 47(1); 64–69, (1976). https://doi.org/10.1063/1.322296
2. Vargas, H., Miranda, L.C.M. Photoacoustic and related photothermal techniques. Phys. Rep., 161(2); 43–101, (1988). https://doi.org/10.1016/0370-1573(88)90100-7
3. Bialkowski, S. Photothermal Spectroscopy Methods for Chemical Analysis (New York: John Wiley 1996). ISBN: 978-0-471-57467-5
4. Rousset, G., Lepoutre, F., Bertrand, L. Influence of thermoelastic bending on photoacoustic experiments related to measurements of thermal diffusivity of metals. J. Appl. Phys, 54(5) 2383–2391, (1983). https://doi.org/10.1063/1.332352
5. Todorovic D.M., Nikolic P.M., Carrier transport contribution to thermoelastic and electronic deformation in semiconductors, Chapter 9 in Mandelis A. P. Hess, ed. Semiconductors and Electronic Materials, SPIE Opt.Eng .Press, Belingham,Washington, (2000). ISBN: 9780819435064
6. Todorović, D.M., Galović, S., Popović, M. Optically excited plasmaelastic waves in semiconductor plate-coupled plasma and elastic phenomena. J. Phys.: Conf. Ser 214, 012106, (2010). https://doi.org/10.1088/1742-6596/214/1/012106
7. Galović, S., Popović, M., Todorović, D.M. Photothermal dynamic elastic bending in a semiconductor circular plate induced by a focused laser beam. Journal of Physics: Conference Series, 214, 012113. (2010) https://doi.org/10.1088/1742-6596/214/1/012113
8. Wang, X., Xu, X., Thermoelastic wave induced by pulsed laser heating. Appl. Phys. A 73, 107–114, (2001). https://doi.org/10.1007/s003390000593
9. Wang, X., Xu, X.,Thermoelastic wave in metal induced by ultrafast laser pulses. J. Therm. Stresses 25, 457–473, (2002). https://doi.org/10.1080/01495730252890186
10. Todorović, D.M., Cretin, B., Vairac, P., Song, Y.Q., Rabasović, M.D., Markushev, D.D, Laser-Excited Electronic and Thermal Elastic Vibrations in a Semiconductor Rectangular Plate. Int J Thermophys., 34(8-9); 1712–1720, (2013) https://doi.org/10.1007/s10765-013-1461-8
11. Nesic, M.V., Popovic, M.N., Galovic, S.P., Djordjevic, K.Lj., Jordovic-Pavlovic, M.I., Miletic, V.V., Markushev, D.D., Estimation of linear expansion coefficient and thermal diffusivity by photoacoustic numerical self-consistent procedure. J. Appl. Phys. 131(10); 105104, (2022) https://doi.org/10.1063/5.0075979
12. Wang, X., Pang, Y., Ku, G., Xie, X., Stoica, G., Wang, L.V. Noninvasive laser-induced photoacoustic tomography for structural and functional in vivo imaging of the brain. Nat. Biotechnol., 21(7); 803–806, (2003) https://doi.org/10.1038/nbt839
13. Xu, M., Wang, L.V. Photoacoustic imaging in biomedicine. Rev. Sci. Instrum., 77(4); 041101, (2006) http://dx.doi.org/10.1063/1.2195024

14. Todorovi D.M., Cretin B., Song Y.Q., Vairac P. Photothermal elastic vibration method: Investigation of the micro-electro-mechanicalsystems, J. Phys.: Conf. Ser. 214 012105 15th International Conference on Photoacoustic and Photothermal Phenomena (ICPPP15) (2010). https://doi.org/10.1088/1742-6596/214/1/012105

15. Cyr B., Sumaria V., Long Y., Tadigadapa S., Sugawara T., Fu K., How Lasers Exploit Photoacoustic and PhotoelectricPhenomena to Inject Signals into MEMS Microphones, (2024). https://doi.org/10.21203/rs.3.rs-4197809/v1

16. Fang, D.N., Sun, Y.X., Soh, A.K., Advances in thermoelastic damping in micro- and nano- mechanical resonators: a review. J. Solid Mech. Mate. Eng. 1 (1), 18–34, (2007). https://doi.org/10.1299/jmmp.1.18

17. Joseph, D.D., Preziosi, L. Heat waves. Rev. Mod. Phys., 61(1); 41–73, (1989). https://doi.org/10.1103/RevModPhys.61.41

18. Tang, D.W., Araki, N., Wavy, wavelike, diffusive thermal responses of finite rigid slabs to high-speed heating of laser-pulses. Int. J. Heat Mass Trans. 42, 855–860, (1999). https://doi.org/10.1016/s0017-9310(98)00244-0

19. Tang, D.W., Araki, N., The wave characteristics of thermal conduction in metallic films irradiated by ultra-short laser pulses. J. Phys. D: Appl. Phys. 29, 2527–2533, (1996). https://doi.org/10.1088/0022-3727/29/10/001

20. Tzou, D.Y., Macro- to Micro-scale Heat Transfer: The Lagging Behavior. Taylor & Francis, Bristol, (1997). ISBN:9781118818220, https://doi.org/10.1002/9781118818275

21. Ozisik, M.N., Tzou, D.Y., On the wave theory in heat-conduction. J. Heat Transfer ASME 116, 526–535, (1994). https://doi.org/10.1115/1.2910903

22. Novikov, A., Harmonic thermal waves in materials with thermal memory. J. Appl. Phys., 81(3); 1067–1072, (1997). https://doi.org/10.1063/1.363849

23. S. Galovic, D. Kostoski. Photothermal wave propagation in media with thermal memory. J. App. Phys. 93(5); 3063-3070, (2003). https://doi.org/10.1063/1.1540741

24. Lord, H.W., Shulman, Y., A generalized dynamical theory of thermoelasticity. J. Mech. Phys. Solids 15, 299–309, (1067). https://doi.org/10.1016/0022-5096(67)90024-5

25. Sherief, H.H., Anwar, M.N., Problem in generalized thermoelasticity. J. Therm. Stresses 9, 165–181, (1986). https://doi.org/10.1080/01495738608961895

26. Sun, Y.X., Fang, D.N., Soh, A.K., Thermoelastic damping in micro-beam resonators. Int. J. Solids Struct. 43, 3213–3229, (2006). https://doi.org/10.1016/j.ijsolstr.2005.08.011

27. Sun, Y.; Fang, D.; Saka, M.; Soh, A.K. Laser-induced vibrations of micro-beams under different boundary conditions. Int. J. Solids Struct. 45, 1993–2013, (2008). https://doi.org/10.1016/j.ijsolstr.2007.11.006

28. Stanimirović, Z., Stanimirović, I., Galović, S., Djordjević, K., Suljovrujić, E. Transmission pulse photoacoustic response of thin semiconductor plate, J. Appl. Phys. 133,195701 (2023). https://doi.org/10.1063/5.0152714

29. Galovic, S.P., Stanimirovic, Z., Stanimirovic, I., Djordjevic, K.L., Milicevic, D., Suljovrujic, E. Time-resolved photoacoustic response of thin solids measured using minimal volume cell. Int. Commun. Heat Mass Transf. 155, 107574, (2024). https://doi.org/10.1016/j.icheatmasstransfer.2024.107574

30. Djordjevic, K.Lj., Galovic, S.P., Nesic, M.V., Todorovic, D.M., Popovic, M.N., Markushev, D.D., Markushev, D.K. Transmission pulse photoacoustic set-up for characterization of solids, in 21st International Symposium INFOTEH-JAHORINA, 16-18 (March 2022). https://infoteh.etf.ues.rs.ba/zbornik/2022/radovi/O-8-3.pdf

31. Galovic, S.P., Djordjevic, K.Lj, Nesic, M.V., Popovic, MN, Markushev, DD Markushev, DK, Todorovic, DM, Time-domain minimum-volume cell photoacoustic of thin semiconductor layer. I. Theory, J. Appl. Phys. 133,245701, (2023) https://doi.org/10.1063/5.0152519

32. Galovic, S., Soskic, Z., Popovic, M.,Cevizovic, D., Stojanovic, Z., Theory of photoacoustic effect in media with thermal memory, J. Appl. Phys. 116(2),024901,2014 https://doi.org/10.1063/1.4885458

33. Mitra, K., Kumar, S., Vedavarez, A., Moallemi. M.K., Experimental Evidence of Hyperbolic Heat Conduction in Processed Meat. J. Heat Transfer, 117(3); 568-573, (1995) https://doi.org/10.1115/1.2822615

34. Stanimirović, I, Markushev, D., Stanimirović, Z, Galović, S, Djordjević, K. Analysis of plasma-elastic component of time-domain photoacoustic response, J. Appl. Phys. 133, 235701, (2023). https://doi.org/10.1063/5.0152713

35. Lashkevych I, Titov O., Gurevich Y.G. Recombination and temperature distribution in semiconductors, IOP Publishing Ltd, Semicond. Sci. Technol. 27, 055014, (2012). https://doi.org/10.1088/0268-1242/27/5/055014

36. Mandelis A. Laser infrared photothermal radiometry of semiconductors: principles and applications to solid state electronics. Solid-State Electronics, 42(1), 1–15, (1998). https://doi.org/10.1016/s0038-1101(97)00238-4

37. Rojas-Trigos J.B., Calderón A., Marín E. A practical model for the determination of transport parameters in semiconductors. Journal of Materials Science, 46(24), 7799–7805 (2011), https://doi.org/10.1007/s10853-011-5760-9

38. Belajcic, D. Differential equation (in Serbian), Naucna knjiga, Belgrade, (1989)

39. Todorovi D.M., Nikolic P.M., Carrier transport contribution to thermoelastic and electronic deformation in semiconductors, Chapter 9 in Mandelis A. P. Hess, ed. Semiconductors and Electronic   Materials, SPIE Opt.Eng .Press, Belingham,Washington, 2000. ISBN: 9780819435064

40. Stojic, M., Continuous System of Automatic Control (in Serbian), (Naucna knjiga, Belgrade, 1991.)

41. Stanimirovic, Z., Stanimirovic, I, Galovic, S., Djordjevic, K., Suljovrujic, E. Haar wavelet operational matrix based numerical inversion of Laplace transform for irrational and transcendental transfer functions. Facta universitatis - series: Electronics and Energetics. 2023, 3, Issue 3, 395-410. https://doi.org/10.2298/FUEE2303395S